ROYAL SOCIETY OPEN SCIENCE

royalsocietypublishing.org/journal/rsos

Research

Cite this article: Adamatzky A. 2018 On discovering functions in actin filament automata. *R. Soc. open sci.* **6**: 181198.
http://dx.doi.org/10.1098/rsos.181198

Received: 19 July 2018
Accepted: 12 December 2018

Subject Category:
Computer science

Subject Areas:
molecular computing/theory of computing/biomimetics

Keywords:
actin, computing, automata

Author for correspondence:
Andrew Adamatzky
e-mail: andrew.adamatzky@uwe.ac.uk

THE ROYAL SOCIETY PUBLISHING

On discovering functions in actin filament automata

Andrew Adamatzky

Unconventional Computing Lab, University of the West of England, Bristol, UK

AA, 0000-0003-1073-2662

We simulate an actin filament as an automaton network. Every atom takes two or three states and updates its state, in discrete time, depending on a ratio of its neighbours in some selected state. All atoms/automata simultaneously update their states by the same rule. Two state transition rules are considered. In semi-totalistic Game of Life like actin filament automaton atoms take binary states '0' and '1' and update their states depending on a ratio of neighbours in the state '1'. In excitable actin filament automaton atoms take three states: resting, excited and refractory. A resting atom excites if a ratio of its excited neighbours belong to some specified interval; transitions from excited state to refractory state and from refractory state to resting state are unconditional. In computational experiments, we implement mappings of an 8-bit input string to an 8-bit output string via dynamics of perturbation/excitation on actin filament automata. We assign eight domains in an actin filament as I/O ports. To write True to a port, we perturb/excite a certain percentage of the nodes in the domain corresponding to the port. We read outputs at the ports after some time interval. A port is considered to be in a state True if a number of excited nodes in the port's domain exceed a certain threshold. A range of eight-argument Boolean functions is uncovered in a series of computational trials when all possible configurations of eight-elements binary strings were mapped onto excitation outputs of the I/O domains.

1. Introduction

Ideas of information processing on a cytoskeleton network have been proposed by Hameroff and Rasmussen in late 1980s in their designs of tubulin microtubules automata [1] and a general framework of cytoskeleton automata as sub-cellular information processing networks [2,3]. Priel, Tuszynski and Cantiello developed a detailed concept on how information processing could be implemented in actin-tubulin networks of neuron dendrites [4]. A signal transmission along the microtubules is implemented via travelling localized patterns of conformation changes or orientations of dipole moments of the tubulin units

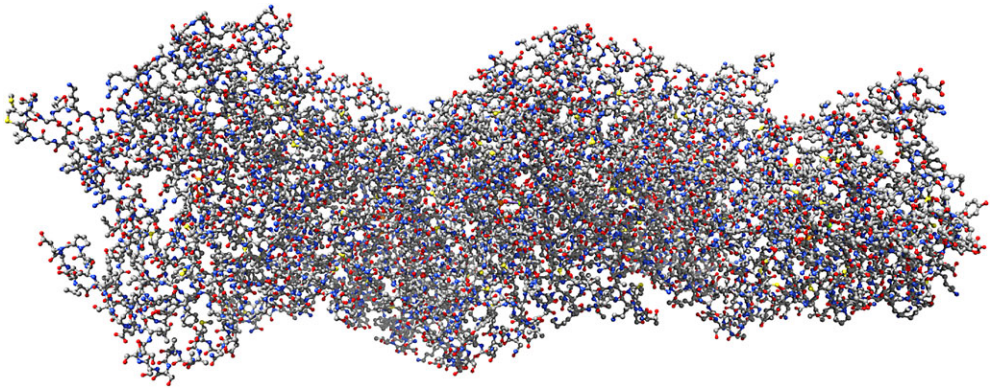

Figure 1. A pseudo-atomic model of F-actin [27] in Corey–Pauling–Kolun colouring.

in tubulin microtubules and ionic waves in actin filaments. A high likelihood of existence of travelling localizations (defects, ionic waves and solitons) in tubulin microtubules and actin filaments is supported by a range of independent (bio)-physical models [5–12]. A convincing hypothesis is that actin networks in synaptic formations play a role of filtering/processing input information which is further conveyed to and amplified by tubulin microtubules. Thus, in the present paper we focus on actin filaments.

Actin is a protein presented in all eukaryotic cells in forms of globular actin (G-actin) and filamentous actin (F-actin) [13–15]. G-actin polymerizes in double helix of filamentous actin; during polymerization G-actin units slightly change their shapes and thus become F-actin units [16]. The actin networks play a key role in information processing [17–20] in living cells. Previously, we have demonstrated how to implement Boolean, multi-valued and quantum logical gates on coarse-grained models of actin filaments using cellular automata, quantum automata and a lattice with Morse potential approaches [21–25]. Theoretical designs of actin-based logical circuits realize logical gates via collisions between travelling localizations. Such an approach assumes that we can address nearly every atom in the actin molecule [26] or control exact timing of the collisions between travelling localizations [25]. Such assumptions might prove to be unrealistic when experimental laboratory implementations are concerned. This is why, in the present paper, we consider a less restrictive, than in previous implementations, way of executing computation on protein polymer: to probe relatively large portions of an actin filament as I/O and uncover Boolean functions implemented via input to output mapping. The approach proposed is novel and has not been considered before. Another original feature of the presented results is that we employ a detailed model of several actin units arranged in the helix. The model is introduced in §2. To discover Boolean functions implementable in the actin filament, we split the helix into eight domains. We perturb the domains in all possible combinations of excitation representing the state of 8-bit strings and record their outputs. A mapping between an input and output sets of binary strings is constructed then. This is shown in §3. We discuss limitations of the approach and future developments in §4.

2. Actin filament automata

We employed a pseudo-atomic model of an F-actin filament (figure 1) reconstructed by Galkin *et al*. [27] at 4.7 Å resolution using a direct electron detector, cryoelectron microscopy and the forces imposed on actin filaments in thin films.[1] The model has 14 800 atoms and is composed of six F-actin molecules. Following our previous convention [28], we represent an F-actin filament as a graph $\mathcal{F} = \langle \mathbf{V}, \mathbf{E}, \mathbf{C}, \mathbf{Q}, f \rangle$, where $\mathbf{V}$ is a set of nodes, $\mathbf{E}$ is a set of edges, $\mathbf{C}$ is a set of Euclidean coordinates of nodes from $\mathbf{V}$, $\mathbf{Q}$ is a set of node states, $f : \mathbf{Q} \times [0,1] \rightarrow \mathbf{Q}$ is a node state transition function, calculating next state of a node depending on its current state and a ratio of excited neighbours belonging to a sub-interval of $[0, 1]$. Each atom from a pseudo-atomic model of an F-actin filament is represented by a node from $\mathbf{V}$ with its three-dimensional coordinates being a member of $\mathbf{C}$; atomic

[1]PDB file can be downloaded here https://www.rcsb.org/structure/3J8I.

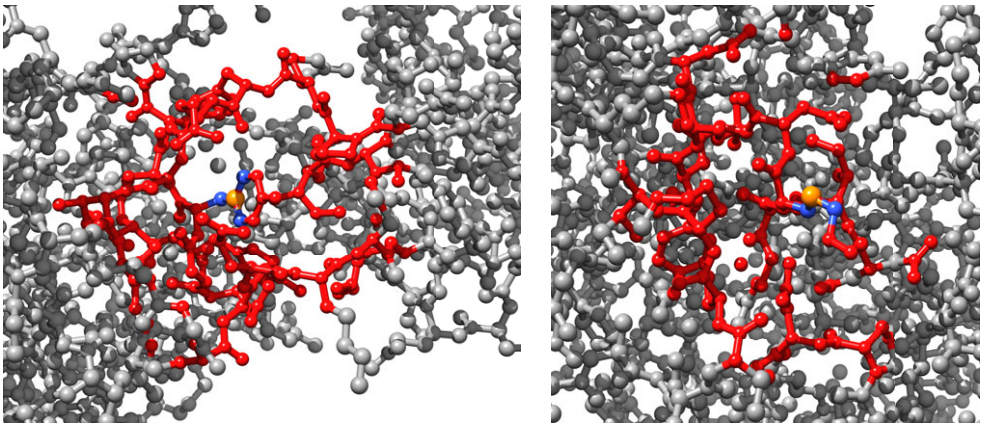

Figure 2. Examples of neighbourhoods. Central nodes, 'owners' of the neighbourhoods are coloured orange, their hard neighbours are blue and their soft neighbours are red.

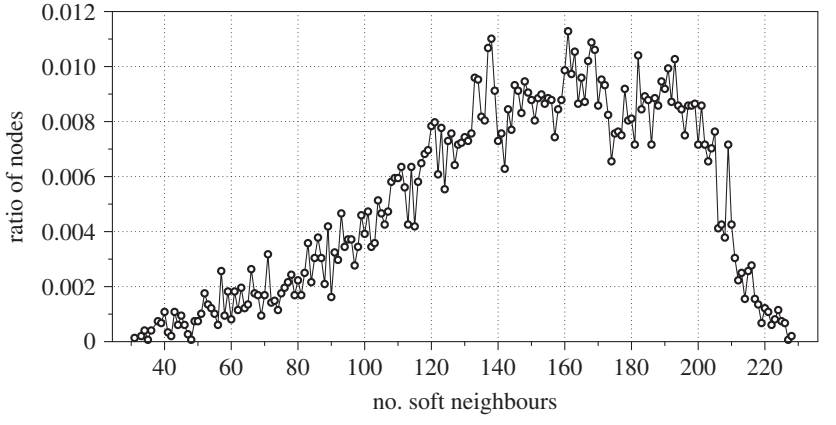

Figure 3. Distribution of a ratio of nodes versus numbers of their soft neighbours, $\rho = 10$.

bonds are represented by **E**. Each node $p \in \mathbf{V}$ takes states from a finite set **Q**. All nodes update their states simultaneously in discrete time. A node p updates its state depending on its current state p^t and ratio $\gamma(p)^t$ of its neighbours being in some selected state ★. We consider two types of a node neighbour. Let $u(p)$ be nodes from **V** that are connected with an edge with a node p; they correspond to atoms connected by the chemical bonds with atom p. We call them hard neighbours because their neighbourhood is determined by the chemical structure of F-actin. The ratio of nodes with one hard neighbour is 0.298, two hard neighbours 0.360, three hard neighbours 0.341 and four hard neighbours 0.001.

The actin molecule is folded in the three-dimensional Euclidean space. Let δ be an average distance between two hard neighbours, for F-actin $\delta = 1.43$ Å units. Let $w(p)$ be the set of nodes of $\mathcal{F}$ that are at distance not exceed ρ, in the Euclidean space, from node p. We call them soft neighbours because their neighbourhood is determined by the three-dimensional structure of F-actin. Thus, each node p has two neighbourhoods: hard neighbourhood $u(p) = \{s \in \mathbf{V}{:}(ps) \in \mathbf{E}\}$ (actin automata with hard neighbourhood were firstly proposed by us in [28]), and soft neighbourhood $w(p) = \{s \in \mathbf{V}{:}s \notin u(p)$ and $d(c_p, c_s) \leq \rho\}$, where $d(c_p, c_s)$ is a distance between nodes p and s in three-dimensional Euclidean space and $c_s, c_p \in \mathbf{C}$. Interactions between a node and its hard neighbours takes place via atomic bounds and via the node and its soft neighbours via ionic currents. We have chosen $\rho = 10$ Å, which is seven times more than an average Euclidean distance 1.42 Å between two hard neighbours. Examples of neighbourhoods are shown in figure 2. The distribution of a number of soft neighbours versus a ratio of nodes with such number of soft neighbours is shown in figure 3; nearly half of the nodes (ratio 0.45) has from 133 to 185 neighbours. The ratio $\gamma(p)^t$ is calculated as $\gamma(p)^t = |s \in u(p){:}s^t = \bigstar| + \mu \cdot |s \in w(p){:}s^t = \bigstar|/|u(p)| + |w(p)|$, where $|\mathbf{S}|$ is a number of elements in the set **S** and μ is a weight of soft neighbours; we used $\mu = 0.9$ in experiments reported.

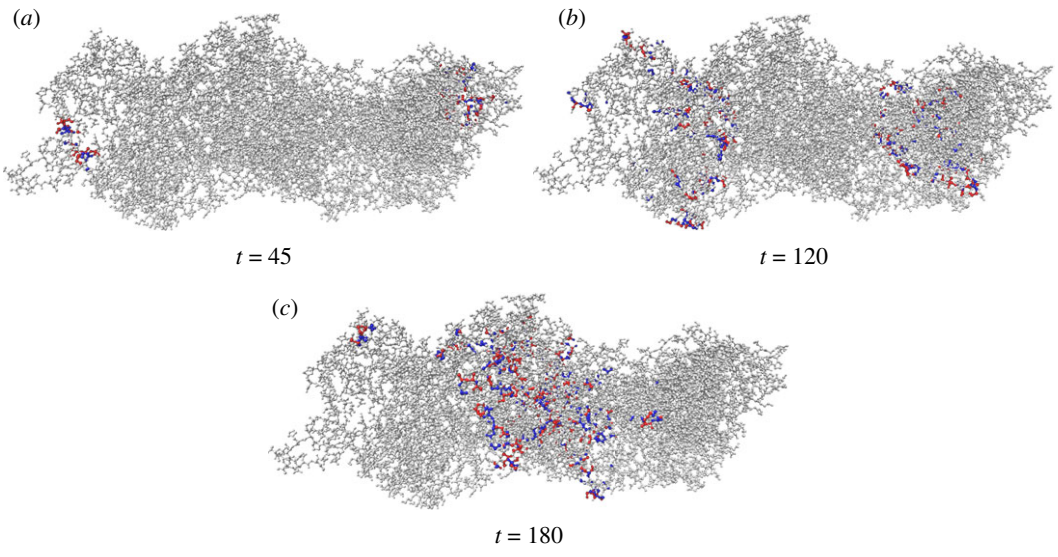

Figure 4. Annihilation of excitation wave-fronts in $\mathcal{E}$ for $[\theta'_\circ, \theta''_\circ] = [0.125, 1]$.

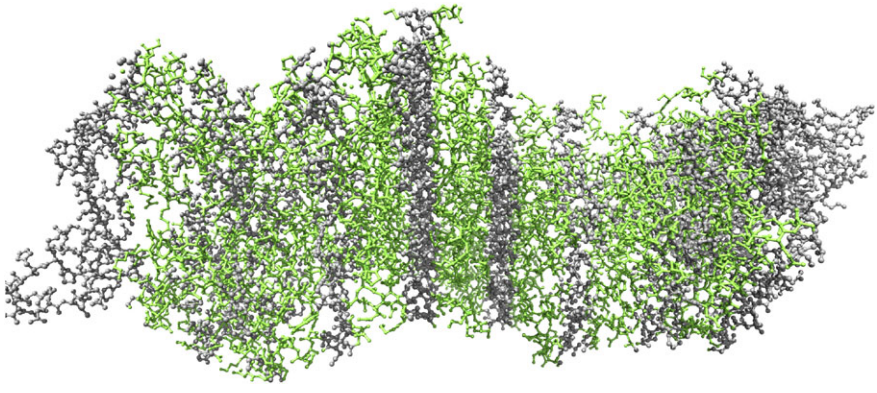

Figure 5. Nodes of I/O domains $D_0 \ldots D_7$ are shown by green colour.

We consider two species of family $\mathcal{F}$: semi-totalistic automaton $\mathcal{G} = \langle \mathbf{V}, \mathbf{E}, \mathbf{C}, \{\bigstar, \circ\}, f^G \rangle$ and excitable automaton $\mathcal{E} = \langle \mathbf{V}, \mathbf{E}, \mathbf{C}, \{\bigstar, \circ, \bullet\}, f^E \rangle$. The rules f^G and f^E are defined as follows:

$$p^{t+1} = f^G(p) = \begin{cases} \bigstar, & \text{if } ((p^t = \circ) \wedge (\theta'_\circ \le \gamma(p)^t \le \theta''_\circ)) \vee ((p^t = \bigstar) \wedge (\theta'_\bigstar \le \gamma(p)^t \le \theta''_\bigstar)) \\ \circ, & \text{otherwise} \end{cases} \tag{2.1}$$

$$p^{t+1} = f^E(p) = \begin{cases} \bigstar, & \text{if } ((p^t = \circ) \wedge (\theta'_\circ \le \gamma(p)^t \le \theta''_\circ)) \\ \bullet, & \text{if } p^t = \circ \\ \circ, & \text{otherwise.} \end{cases} \tag{2.2}$$

We have chosen intervals $[\theta'_\circ, \theta''_\circ] = [\theta'_\bigstar, \theta''_\bigstar] = [0.25, 0.375]$ for $\mathcal{G}$ and $[\theta'_\circ, \theta''_\circ] = [0.15, 0.25]$ for $\mathcal{E}$ because they support localized modes of excitation, i.e. a perturbation of the automata at a single site or a compact domain of several sites does not lead to an excitation spreading all over the actin chain. Localized excitations emerged at different input domains can interact with other and the results of their interactions in the output domains will represent values of a logical function computed.

Automaton $\mathcal{G}$ is a Game of Life like automaton [29,30]. Speaking in the Game of Life lingo we can say that a dead node $\circ$ becomes alive $\bigstar$ if a ratio of live nodes in its neighbourhood lies inside interval $[\theta'_\circ, \theta''_\circ]$; a live node $\bigstar$ remains alive if a ratio of live nodes in its neighbourhood lies inside interval $[\theta'_\bigstar, \theta''_\bigstar]$. Automaton $\mathcal{E}$ is a Greenberg–Hastings [31] like automaton: a resting node $\circ$ excites if a ratio of excited nodes in its neighbourhood lies inside interval $[\theta'_\circ, \theta''_\circ]$; and excited node $\bigstar$ takes refractory state $\bullet$ in

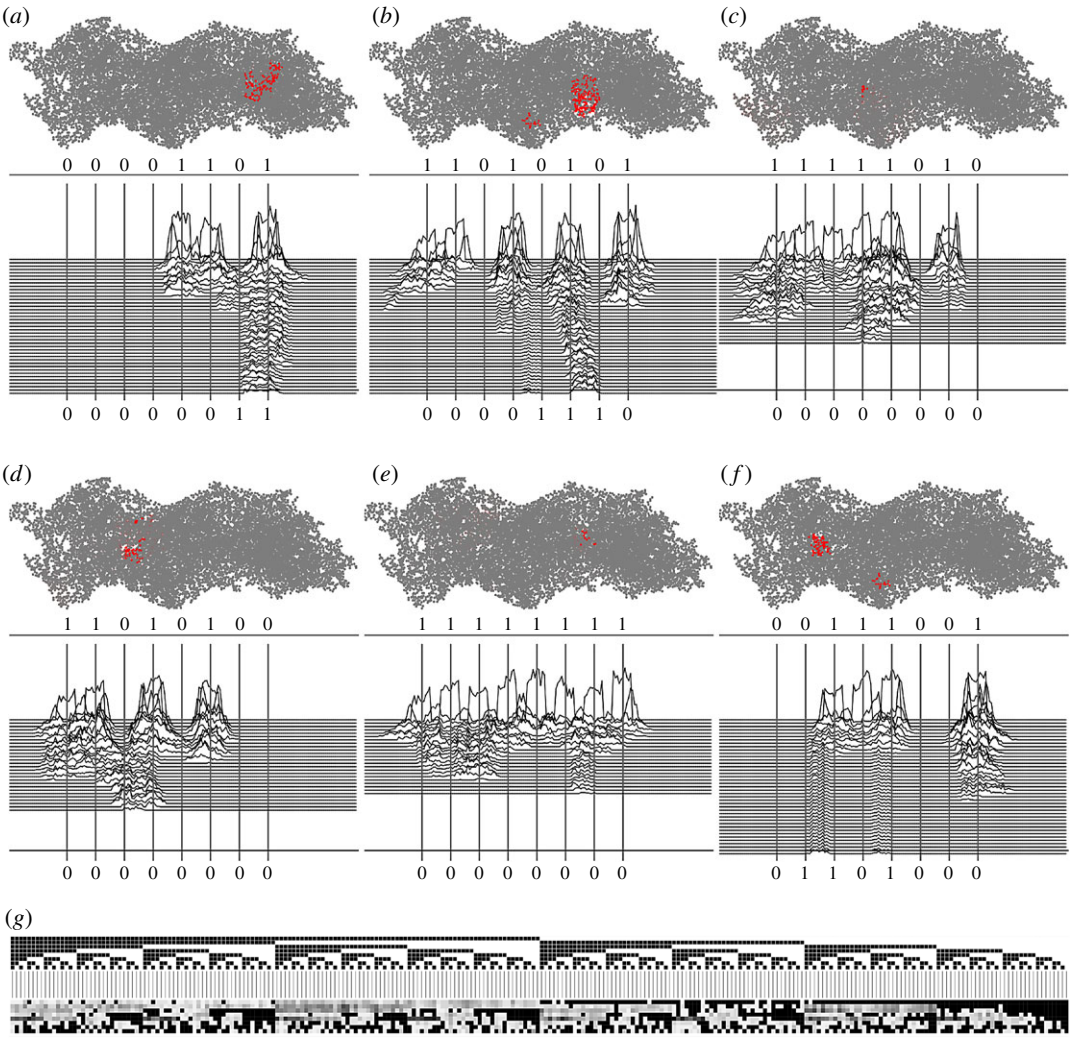

Figure 6. Discovering Boolean functions in automaton $\mathcal{G}$. (a–f) Examples of excitation dynamics in automaton $\mathcal{G}$, $\theta'_{\circ} = \theta'_{\bigstar} = 0.25$ and $\theta''_{\circ} = \theta''_{\bigstar} = 0.375$. Projection of actin filament on z-plane is shown in grey; projection of nodes being in state ★ by the moment of recording inputs are shown in red. Plots show values of activity, i.e. a number of nodes in state ★ along the x-coordinate. See videos of experiments at https://doi.org/10.5281/zenodo.1312141. (g) Visualization of register mapping implemented by automaton $\mathcal{G}$.

Table 1. Fragment of experimentally obtained mapping **S** to **W** for automaton $\mathcal{G}$.

$(I_0I_1I_2I_3I_4I_5I_6I_7)$	w_0	w_1	w_2	w_3	w_4	w_5	w_6	w_7
1011100	0	0	0.01	0.01	0.14	0.03	0.01	0
1011101	0.01	0.03	0.01	0.01	0.2	0.03	0.01	0.03
1011110	0	0	0	0	0.14	0.02	0.01	0.01
1011111	0	0.01	0.01	0.02	0.25	0.04	0.02	0.02
1100000	0	0.04	0.04	0	0	0	0	0
1100001	0	0.02	0.02	0	0	0	0	0.01
1100010	0	0.03	0.05	0	0	0.01	0.02	0
1100011	0	0.05	0.03	0	0	0	0	0.02
1100100	0	0.06	0.04	0	0	0.02	0	0
1100101	0.01	0.06	0.04	0	0	0.04	0.03	0.02

Table 2. Functions implemented by (*a*) $\mathcal{G}$ automaton, $\theta'_\circ = \theta'_\star = 0.25$ and $\theta''_\circ = \theta''_\star = 0.375$, and (*b*) $\mathcal{E}$ automaton, $\theta'_\circ = 0.15$ and $\theta''_\circ = 0.25$. for various values of reliability threshold γ.

γ	functions
(*a*)	
0.15	$O_1 = I_0 \cdot \overline{I_1} \cdot I_2 \cdot \overline{I_3} \cdot I_4 \cdot I_5 \cdot I_6 \cdot I_7$;
	$O_2 = \overline{I_0} \cdot \overline{I_1} \cdot I_2 \cdot I_3 \cdot I_7 \cdot (I_4 \cdot I_5 \cdot \overline{I_6} + I_4 \cdot \overline{I_5} \cdot I_6 + \overline{I_4} \cdot I_5 \cdot I_6)$;
	$O_4 = \overline{I_0} \cdot \overline{I_1} \cdot \overline{I_2} \cdot I_3 \cdot I_4 \cdot (\overline{I_5} \cdot \overline{I_7} + I_6 \cdot I_7 + I_5 \cdot I_6 \cdot \overline{I_7})$
0.2	$O_4 = I_3 \cdot I_4 \cdot (\overline{I_0} \cdot I_1 \cdot \overline{I_2} \cdot I_5 \cdot I_7 + \overline{I_0} \cdot I_2 \cdot \overline{I_5} \cdot \overline{I_6} \cdot \overline{I_7} + I_0 \cdot \overline{I_1} \cdot \overline{I_2} \cdot \overline{I_5} \cdot I_6 + \overline{I_0} \cdot I_1 \cdot I_2 \cdot \overline{I_5} \cdot I_6 \cdot$
	$\overline{I_7} + I_0 \cdot I_1 \cdot I_2 \cdot \overline{I_5} \cdot I_6 \cdot I_7 + I_0 \cdot \overline{I_1} \cdot \overline{I_2} \cdot \overline{I_5} \cdot \overline{I_6} \cdot I_7 + \overline{I_0} \cdot \overline{I_1} \cdot \overline{I_2} \cdot I_5 \cdot I_6 \cdot \overline{I_7} + \overline{I_0} \cdot \overline{I_1} \cdot \overline{I_2} \cdot \overline{I_5} \cdot I_6 \cdot I_7)$
0.22	$O_4 = \overline{I_2} \cdot I_3 \cdot I_4 \cdot (\overline{I_0} \cdot I_1 \cdot I_5 \cdot I_6 \cdot I_7 + \overline{I_0} \cdot \overline{I_1} \cdot \overline{I_5} \cdot \overline{I_6} \cdot \overline{I_7} + I_0 \cdot \overline{I_1} \cdot \overline{I_5} \cdot \overline{I_6} \cdot I_7 + \overline{I_0} \cdot \overline{I_1} \cdot I_5 \cdot I_6 \cdot$
	$\overline{I_7} + \overline{I_0} \cdot \overline{I_1} \cdot \overline{I_5} \cdot I_6 \cdot I_7)$
0.23	$O_4 = \overline{I_0} \cdot \overline{I_2} \cdot I_3 \cdot I_4 \cdot (\overline{I_1} \cdot I_5 \cdot I_6 \cdot \overline{I_7} + \overline{I_1} \cdot \overline{I_5} \cdot I_6 \cdot I_7 + I_1 \cdot I_5 \cdot I_6 \cdot I_7 + \overline{I_1} \cdot \overline{I_5} \cdot \overline{I_6} \cdot \overline{I_7})$
0.24	$O_4 = \overline{I_0} \cdot \overline{I_2} \cdot I_3 \cdot I_4 \cdot I_6 \cdot I_7 \cdot (\overline{I_1} \cdot \overline{I_5} + I_1 \cdot I_5)$
0.25	$O_4 = \overline{I_0} \cdot I_1 \cdot \overline{I_2} \cdot I_3 \cdot I_4 \cdot I_5 \cdot I_6 \cdot I_7$
(*b*)	
0.7	$O_0 = \overline{I_0} \cdot I_1 \cdot \overline{I_2} \cdot I_7 \cdot (\overline{I_3} \cdot \overline{I_4} \cdot I_5 \cdot \overline{I_6} + I_3 \cdot I_4 \cdot \overline{I_5} \cdot I_6)$
	$O_1 = I_0 \cdot \overline{I_1} \cdot I_2 \cdot \overline{I_3} \cdot I_4 + \overline{I_0} \cdot I_1 \cdot \overline{I_2} \cdot I_3 \cdot I_4 \cdot \overline{I_5} \cdot I_7 + \overline{I_0} \cdot I_1 \cdot \overline{I_2} \cdot I_3 \cdot \overline{I_4} \cdot I_5 \cdot \overline{I_6} + \overline{I_0} \cdot I_1 \cdot \overline{I_2} \cdot I_3 \cdot \overline{I_4} \cdot I_6 \cdot$
	$\overline{I_7} + \overline{I_0} \cdot I_1 \cdot I_2 \cdot \overline{I_3} \cdot I_4 \cdot \overline{I_5} \cdot \overline{I_6} \cdot I_7 + \overline{I_0} \cdot I_1 \cdot I_2 \cdot \overline{I_3} \cdot I_4 \cdot I_5 \cdot I_6 \cdot I_7 + I_0 \cdot \overline{I_1} \cdot I_2 \cdot I_3 \cdot \overline{I_4} \cdot I_5 \cdot \overline{I_6} \cdot I_7 + \overline{I_0} \cdot$
	$I_1 \cdot \overline{I_2} \cdot I_3 \cdot \overline{I_4} \cdot I_5 \cdot I_6 \cdot I_7$
	$O_2 = I_0 \cdot \overline{I_1} \cdot I_2 \cdot \overline{I_3} \cdot I_4 + \overline{I_0} \cdot I_1 \cdot I_2 \cdot \overline{I_3} \cdot I_4 \cdot \overline{I_5} + I_0 \cdot \overline{I_1} \cdot I_2 \cdot I_3 \cdot \overline{I_4} \cdot I_5 \cdot \overline{I_7} + \overline{I_0} \cdot I_1 \cdot \overline{I_2} \cdot$
	$I_3 \cdot \overline{I_4} \cdot I_6 \cdot \overline{I_7} + \overline{I_0} \cdot I_1 \cdot \overline{I_2} \cdot I_3 \cdot \overline{I_4} \cdot \overline{I_6} \cdot I_7 + \overline{I_0} \cdot I_1 \cdot I_3 \cdot \overline{I_4} \cdot I_5 \cdot \overline{I_6} \cdot \overline{I_7} + \overline{I_0} \cdot I_1 \cdot \overline{I_2} \cdot I_3 \cdot I_4 \cdot \overline{I_5} \cdot$
	$\overline{I_6} \cdot I_7 + I_0 \cdot I_1 \cdot \overline{I_2} \cdot I_3 \cdot \overline{I_4} \cdot I_5 \cdot \overline{I_6} \cdot I_7 + I_0 \cdot \overline{I_1} \cdot I_2 \cdot I_3 \cdot \overline{I_4} \cdot I_5 \cdot \overline{I_6} \cdot I_7 + \overline{I_0} \cdot I_1 2 \cdot I_3 \cdot \overline{I_4} \cdot$
	$I_5 \cdot \overline{I_6} \cdot I_7 + \overline{I_0} \cdot I_1 \cdot I_2 \cdot \overline{I_3} \cdot I_4 \cdot I_5 \cdot I_6 \cdot \overline{I_7} + \overline{I_0} \cdot I_1 \cdot \overline{I_2} \cdot I_3 \cdot \overline{I_4} \cdot I_5 \cdot I_6 \cdot I_7$
	$O_3 = I_2 \cdot \overline{I_3} \cdot I_4 \cdot \overline{I_5} \cdot \overline{I_6} \cdot I_7 + I_0 \cdot I_3 \cdot \overline{I_4} \cdot I_5 \cdot \overline{I_6} \cdot I_7 + \overline{I_0} \cdot I_1 \cdot I_2 \cdot I_3 \cdot \overline{I_4} \cdot I_5 \cdot \overline{I_7} + \overline{I_0} \cdot I_1 \cdot I_3 \cdot \overline{I_4} \cdot I_5 \cdot$
	$\overline{I_6} \cdot I_7 + \overline{I_1} \cdot I_2 \cdot I_3 \cdot \overline{I_4} \cdot I_5 \cdot I_6 \cdot \overline{I_7} + I_0 \cdot \overline{I_1} \cdot I_2 \cdot \overline{I_3} \cdot I_4 \cdot \overline{I_5} \cdot \overline{I_7} + \overline{I_0} \cdot I_1 \cdot I_2 \cdot \overline{I_3} \cdot I_4 \cdot$
	$\overline{I_5} \cdot \overline{I_7} + \overline{I_0} \cdot \overline{I_2} \cdot I_3 \cdot \overline{I_4} \cdot I_5 \cdot I_6 \cdot \overline{I_7} + I_1 \cdot \overline{I_2} \cdot I_3 \cdot \overline{I_4} \cdot I_5 \cdot \overline{I_6} \cdot \overline{I_7} + I_0 \cdot I_1 \cdot \overline{I_2} \cdot I_3 \cdot \overline{I_4} \cdot I_5 \cdot I_6 + I_0 \cdot \overline{I_1} \cdot I_2 \cdot$
	$I_3 \cdot \overline{I_4} \cdot I_5 \cdot \overline{I_6} \cdot \overline{I_7} + \overline{I_0} \cdot \overline{I_1} \cdot I_2 \cdot I_3 \cdot \overline{I_4} \cdot I_5 \cdot \overline{I_6} \cdot I_7 + I_0 \cdot I_1 \cdot I_2 \cdot \overline{I_3} \cdot I_4 \cdot \overline{I_5} \cdot I_6 \cdot \overline{I_7} + I_0 \cdot \overline{I_1} \cdot I_2 \cdot \overline{I_3} \cdot I_4 \cdot \overline{I_5} \cdot$
	$I_6 \cdot I_7 + \overline{I_0} \cdot I_1 \cdot I_2 \overline{I_3} \cdot I_4 \cdot \overline{I_5} \cdot I_6 \cdot I_7 + \overline{I_0} \cdot \overline{I_1} \cdot I_2 \cdot \overline{I_3} \cdot I_4 \cdot \overline{I_5} \cdot \overline{I_6} \cdot \overline{I_7}$
	functions realized on outputs O_4 to O_7 are not shown.
0.8	$O_2 = I_3 \cdot \overline{I_4} \cdot I_5 \cdot I_7 \cdot (\overline{I_0} \cdot I_1 \cdot \overline{I_2} + I_0 \cdot \overline{I_1} \cdot I_2 \cdot \overline{I_6})$
	$O_3 = \overline{I_6} \cdot (I_0 \cdot \overline{I_1} \cdot I_3 \cdot \overline{I_4} \cdot I_5 \cdot I_7 + \overline{I_0} \cdot I_1 \cdot I_3 \cdot \overline{I_4} \cdot I_5 \cdot$
	$I_7 + I_0 \cdot \overline{I_1} \cdot I_2 \cdot I_3 \cdot \overline{I_4} \cdot I_5 \cdot \overline{I_7} + I_0 \cdot \overline{I_1} \cdot I_2 \cdot \overline{I_3} \cdot I_4 \cdot$
	$\overline{I_5} \cdot I_7 + I_0 \cdot I_1 \cdot \overline{I_2} \cdot I_3 \cdot \overline{I_4} \cdot I_5 \cdot I_7)$
	$O_4 = \overline{I_6} \cdot (I_2 \cdot I_3 \cdot \overline{I_4} \cdot I_5 \cdot I_7 + \overline{I_1} \cdot I_2 \cdot \overline{I_3} \cdot I_4 \cdot \overline{I_5} \cdot I_7 + I_0 \cdot I_1 \cdot \overline{I_2} \cdot I_3 \cdot \overline{I_4} \cdot I_5 + I_0 \cdot \overline{I_1} \cdot \overline{I_2} \cdot I_3 \cdot \overline{I_4} \cdot I_5 \cdot I_7)$
	$O_5 = \overline{I_2} \cdot I_3 \cdot \overline{I_4} \cdot I_5 \cdot \overline{I_6} \cdot I_7 \cdot (I_0 + \overline{I_1})$
0.9	$O_5 = \overline{I_1} \cdot I_3 \cdot \overline{I_4} \cdot I_5 \cdot \overline{I_6} \cdot I_7 \cdot (I_0 + \overline{I_2})$

the next step of development, and a refractory • returns to resting state ◦. Rules of Conway's Game of Life could be interpreted as equation (2.1) having perturbation intervals $[\theta'_\circ, \theta''_\circ] = [0.375, 0.375]$ (i.e. exactly value 0.375) and $[\theta'_\star, \theta''_\star] = [0.25, 0.375]$, rules of Greenberg–Hasting automata in terms of equation (2.2) having interval $[\theta'_\circ, \theta''_\circ] = [0.125, 1]$. The exact intervals of perturbation for the Game of Life and the Greenberg–Hasting automata are proven to be not useful for mining functions. This is because $\mathcal{G}$ with the Game of Life interval does not show any sustainable dynamics of excitation, and $\mathcal{E}$ with Greenberg–Hasting interval exhibits 'classical' waves of excitation, where two colliding waves annihilate (figure 4).

The model was implemented in Processing. Data are analysed in Matlab. Patterns of excitation dynamics are visualized in Processing and Chimera.

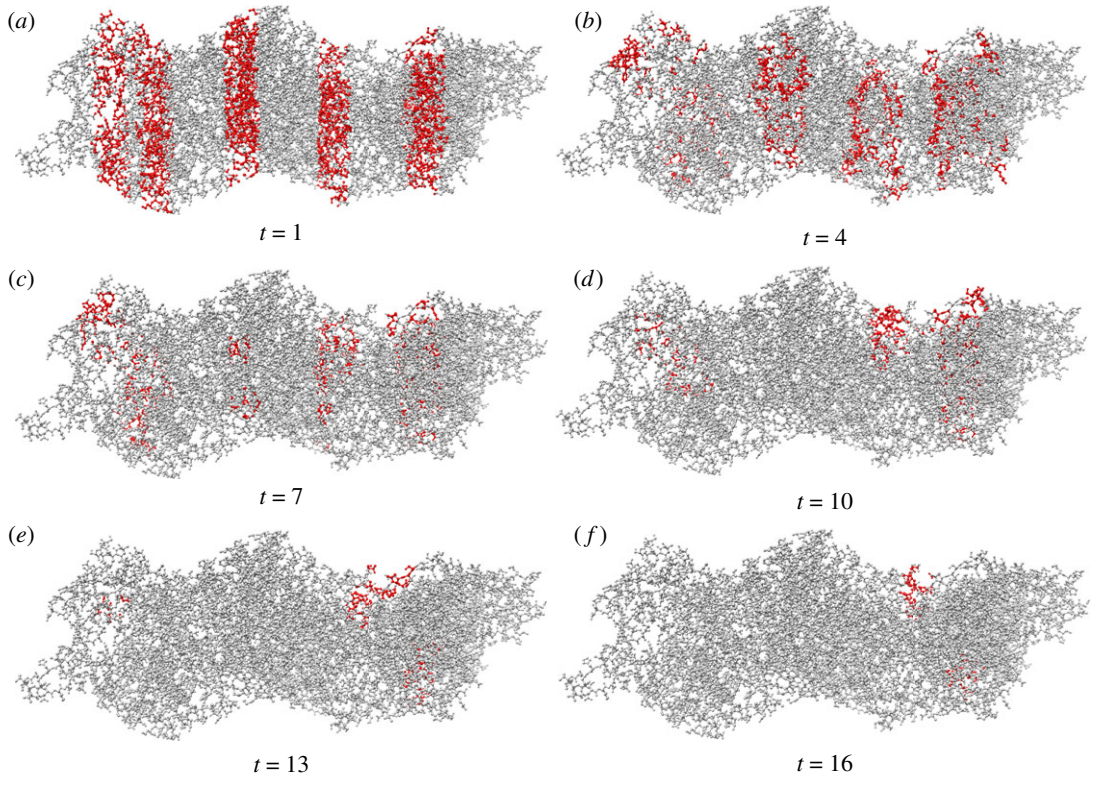

Figure 7. Snapshots of excitation dynamics of automaton $\mathcal{G}$ in response to the input 11010101. See videos of experiments at https://doi.org/10.5281/zenodo.1312141.

3. Discovering functions

We encode Boolean values '0' (False) and '1' (True) in perturbations of selected domains $\boldsymbol{D}$ and extract a range of mappings $\{0,1\}^m \to \{0,1\}^m$, $m \in \boldsymbol{N}$, implementable by the actin filament automaton. Assume input and output tuples $\boldsymbol{I} \in \{0,1\}^m$ and $\boldsymbol{O} \in \{0,1\}^m, m = 8$, the actin automaton implements $\mathbf{I} \to \mathbf{D} \to \mathbf{O}$. We implement computation on actin filament automaton as follows. Eight cylinders across the (xy)-plane with coordinates $D_i = \{p \in \mathcal{V}\colon \mathrm{abs}(p_x - k(i)) < r_s\}$, $0 \le i < 8$, $k(i) = 15 \cdot (i+1)$, are assigned as input–output domains (figure 5). These are mapped onto Boolean inputs $\boldsymbol{I} = (I_0, \ldots, I_7)$ and outputs $\mathbf{O} = (O_0, \ldots, O_7)$ as follows: $I_z = 1$ if $\sum_{p^0 \in D_z} > \kappa$, otherwise $I_z = 0$, and $O_z = 1$ if $\sum_{p^\zeta \in D_z} > \kappa$, otherwise $O_z = 0$; in the present paper we have chosen $\kappa = 0$ and $\zeta = 40$.

Domains from $\mathbf{D}$ at time step $t = 0$ are excited with probability p determined by values of inputs $\mathbf{I}$: if a node p belongs to $\mathbf{D}_i$ and $s_i = 1$ the node takes state $\bigstar$ at the beginning of evolution, $p^0 = \bigstar$ with probability p. We read outputs after $\zeta = 40$ steps of automaton evolution. As soon as 40 iterations occurred ($t = 41$), we measure states of nodes in the domains $\mathbf{D}_i$, $s_i \in \{0,1\}$, and assign outputs depending on the excitation: $O_i = 1$ if $|\{p \in \mathbf{D} : p^t = \bigstar\}| > \kappa$, $\kappa = 0$. Stimulation runs for h trials (repeated simulation of automaton) with all possible configurations of $\boldsymbol{I}$, $h = 100$, where frequencies of outputs are calculated as $W_i = w_i + I_i^T$, $0 \le i < 8$, where T is a trial number, $T = 1, \ldots, h$. By the end of the experiments, we normalize $\mathbf{W}$ as $w_i = w_i/h$, h is the number of trials.

Examples of perturbation dynamics of automaton $\mathcal{G}$ for various input sequences are shown in figure 6*a–f*. Example of a fragment of $\mathbf{W}$ obtained in 100 trials with automaton $\mathcal{G}$ is shown in table 1. Visualization of mapping $\mathbf{S} \to \mathbf{W}$ is presented in figure 6*g*. There, lexicographically ordered elements of $\mathbf{S}$ are shown by black ('1') and white ('0') squares: top row from (0000000) on the right to (11111111) on the left. Corresponding elements of $\mathbf{W}$ are shown by gradations of grey $255 \cdot w_i$. From $\mathbf{W}$, we extract values of outputs $\mathbf{O}$ for various ranges of $\gamma \in [0,1]$ as follows: $O_i = 1$ if $w_i > \gamma$, and $O_i = 0$ otherwise.

Boolean functions, in the form $O_i = f(I_0 \ldots I_7)$, realizable by automata $\mathcal{G}$ and $\mathcal{E}$ are listed in table 2. In automaton $\mathcal{G}$ a ratio ϵ of I/O transitions where at least one element of $\mathbf{W}$ exceeds γ shows quadratic decrease with increase of γ (figures 7 and 8*a*); the same applies to automaton $\mathcal{E}$. This reflects both a decrease in a number of functions realizable on output domains and a decrease of the functions

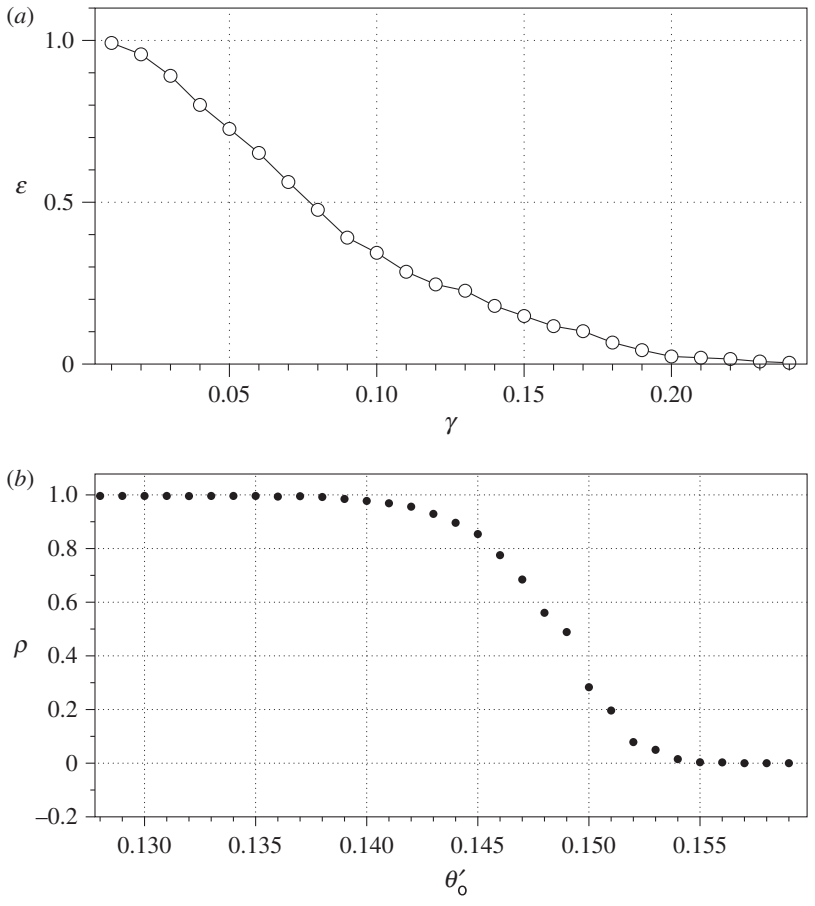

Figure 8. (*a*) Ratio ε of transitions where at least one entry in $\boldsymbol{W}$ exceeds γ. (*b*) Dependence of the ratio ρ of outputs in state 1 to an overall number of outputs of the lower threshold of excitation $\theta'_\circ$; upper threshold $\theta'_\circ = 0.25$ was kept constant.

complexity in terms of the arguments. A number of functions implementable in $\mathcal{F}$ polynomially decrease with increase of $\theta'_\circ$ (figure 8*b*).

4. Discussion

We demonstrated an implementation of logical functions on automaton models of actin filaments. The approach was inspired by the 'evolution in materio' framework [32–34] on implementing computation without knowing the exact physical structure of a computing substrate. Propagating patterns in the Game of Life like automaton $\mathcal{G}$ can be seen as the discrete analogies of vibration excitation [35–38]. The dynamics of Greenberg–Hasting excitable automaton $\mathcal{E}$ is a finite-state machine analogue of the ionic waves, theoretical models of which are well studied in a context of tubulin microtubules and actin filaments [7,10,39–41]. How feasible is the approach? So far there are no experimental data on vibration modes of a single strand, or even a bundle of actin filaments or tubulin tubes, of a cytoskeleton polymer [42]. Outputs of the actin filament processors can be measured using controlled light waves and pulse trains [43–46]. There are ways to measure a vibration of a cell membrane, as demonstrated in [47]. The vibration of the membrane might reflect vibrations of cytoskeleton networks attached to the membrane [48], however it shows a cumulative effect of vibration of a cytoskeleton network. Owing to the polarity of actin units, vibration modes are manifested in electromagnetic perturbation which could be measured when existing experimental techniques are perfected [37,38].

Data accessibility. The data supporting the findings of this study are available at https://doi.org/10.5281/zenodo.1312141.

Authors' contributions. A.A. the principal investigator and corresponding author, directed the research, undertook the research and wrote the manuscript.

Competing interests. We declare we have no competing interests.

Funding. We received no funding for this research.

References

1. Hameroff SR, Rasmussen S. 1989 Information processing in microtubules: biomolecular automata and nanocomputers. In *Molecular electronics* (ed. FT Hong), pp. 243–257. Berlin, Germany: Springer.
2. Rasmussen S, Karampurwala H, Vaidyanath R, Jensen KS, Hameroff S. 1990 Computational connectionism within neurons: a model of cytoskeletal automata subserving neural networks. *Physica D* **42**, 428–449. (doi:10.1016/0167-2789(90)90093-5)
3. Hameroff S, Rasmussen S. 1990 Microtubule automata: sub-neural information processing in biological neural networks. In *Theoretical Aspects of Neurocomputing, Symp. on Neural Networks and Neurocomputing (NEURONET '90), Prague, Czech Republic, 10–14 September*. Singapore: World Scientific.
4. Priel A, Tuszynski JA, Cantiello HF. 2006 The dendritic cytoskeleton as a computational device: an hypothesis. In *The emerging physics of consciousness* (ed. JA Tuszynski), pp. 293–325. Berlin, Germany: Springer.
5. Tuszyński J, Hameroff S, Satarić M, Trpisova B, Nip M. 1995 Ferroelectric behavior in microtubule dipole lattices: implications for information processing, signaling and assembly/disassembly. *J. Theor. Biol.* **174**, 371–380. (doi:10.1006/jtbi.1995.0105)
6. Tuszynski J, Luchko T, Carpenter E, Crawford E. 2004 Results of molecular dynamics computations of the structural and electrostatic properties of tubulin and their consequences for microtubules. *J. Comput. Theoret. Nanosci.* **1**, 392–397. (doi:10.1166/jctn.2004.042)
7. Tuszyński J, Portet S, Dixon J, Luxford C, Cantiello H. 2004 Ionic wave propagation along actin filaments. *Biophys. J.* **86**, 1890–1903. (doi:10.1016/S0006-3495(04)74255-1)
8. Tuszyński J, Brown J, Crawford E, Carpenter E, Nip M, Dixon J, Satarić M. 2005 Molecular dynamics simulations of tubulin structure and calculations of electrostatic properties of microtubules. *Math. Comput. Model.* **41**, 1055–1070.
9. Tuszyński J, Portet S, Dixon J. 2005 Nonlinear assembly kinetics and mechanical properties of biopolymers. *Nonlinear Anal. Theory Methods Appl.* **63**, 915–925. (doi:10.1016/j.na.2005.01.089)
10. Satarić M, Sekulić D, Živanov M. 2010 Solitonic ionic currents along microtubules. *J. Comput. Theoret. Nanosci.* **7**, 2281–2290. (doi:10.1166/jctn.2010.1609)
11. Satarić M, Satarić B. 2011 Ionic pulses along cytoskeletal protophilaments. *J. Phys. Conf. Ser.* **329**, 012009. (doi:10.1088/1742-6596/329/1/012009)
12. Kavitha L, Parasuraman E, Muniyappan A, Gopi D, Zdravković S. 2017 Localized discrete breather modes in neuronal microtubules. *Nonlinear Dyn.* **88**, 2013–2033. (doi:10.1007/s11071-017-3359-7)
13. Straub F. 1943 Actin, ii. *Stud. Inst. Med. Chem. Univ. Szeged* **3**, 23–37.
14. Korn ED. 1982 Actin polymerization and its regulation by proteins from nonmuscle cells. *Physiol. Rev.* **62**, 672–737. (doi:10.1152/physrev.1982.62.2.672)
15. Szent-Györgyi AG. 2004 The early history of the biochemistry of muscle contraction. *J. Gen. Physiol.* **123**, 631–641. (doi:10.1085/jgp.200409091)
16. Oda T, Iwasa M, Aihara T, Maéda Y, Narita A. 2009 The nature of the globular to fibrous-actin transition. *Nature* **457**, 441–445. (doi:10.1038/nature07685)
17. Fifková E, Delay RJ. 1982 Cytoplasmic actin in neuronal processes as a possible mediator of synaptic plasticity. *J. Cell Biol.* **95**, 345–350. (doi:10.1083/jcb.95.1.345)
18. Kim C-H, Lisman JE. 1999 A role of actin filament in synaptic transmission and long-term potentiation. *J. Neurosci.* **19**, 4314–4324. (doi:10.1523/JNEUROSCI.19-11-04314.1999)
19. Dillon C, Goda Y. 2005 The actin cytoskeleton: integrating form and function at the synapse. *Annu. Rev. Neurosci.* **28**, 25–55. (doi:10.1146/annurev.neuro.28.061604.135757)
20. Cingolani LA, Goda Y. 2008 Actin in action: the interplay between the actin cytoskeleton and synaptic efficacy. *Nat. Rev. Neurosci.* **9**, 344–356. (doi:10.1038/nrn2373)
21. Siccardi S, Adamatzky A. 2015 Actin quantum automata: communication and computation in molecular networks. *Nano Commun. Networks* **6**, 15–27. (doi:10.1016/j.nancom.2015.01.002)
22. Siccardi S, Tuszynski JA, Adamatzky A. 2016 Boolean gates on actin filaments. *Phys. Lett. A* **380**, 88–97. (doi:10.1016/j.physleta.2015.09.024)
23. Siccardi S, Adamatzky A. 2016 Quantum actin automata and three-valued logics. *IEEE J. Emerg. Sel. Top. Circ. Syst.* **6**, 53–61. (doi:10.1109/JETCAS.2016.2528722)
24. Siccardi S, Adamatzky A. 2016 Logical gates implemented by solitons at the junctions between one-dimensional lattices. *Int. J. Bifurcation Chaos* **26**, 1650107. (doi:10.1142/S0218127416501078)
25. Siccardi S, Adamatzky A. 2017 Models of computing on actin filaments. In *Advances in unconventional computing* (ed. A Adamatzky), pp. 309–346. Berlin, Germany: Springer.
26. Adamatzky A. 2017 Logical gates in actin monomer. *Sci. Rep.* **7**, 11755. (doi:10.1038/s41598-017-11333-7)
27. Galkin VE, Orlova A, Vos MR, Schröder GF, Egelman EH. 2015 Near-atomic resolution for one state of F-actin. *Structure* **23**, 173–182. (doi:10.1016/j.str.2014.11.006)
28. Adamatzky A. 2017 On dynamics of excitation and information processing in F-actin: automaton model. *Complex Syst.* **2**, 295–317. (doi:10.25088/ComplexSystems)
29. Conway J. 1970 The game of life. *Sci. Am.* **223**, 4.
30. Adamatzky A (ed.) 2010 *Game of life cellular automata*, vol. 1. Berlin, Germany: Springer.
31. Greenberg JM, Hastings S. 1978 Spatial patterns for discrete models of diffusion in excitable media. *SIAM J. Appl. Math.* **34**, 515–523. (doi:10.1137/0134040)
32. Harding S, Miller JF. 2005 Evolution in materio: evolving logic gates in liquid crystal. In *Proc. Eur. Conf. Artif. Life (ECAL 2005), Workshop on Unconventional Computing: From cellular automata to wetware* (ed. A Adamatzky), pp. 133–149, Beckington, UK: Luniver Press.
33. Miller JF, Harding SL, Tufte G. 2014 Evolution-in-materio: evolving computation in materials. *Evol. Intell.* **7**, 49–67. (doi:10.1007/s12065-014-0106-6)
34. Harding S, Koutnik J, Greff K, Schmidhuber J, Adamatzky A. 2016 Discovering Boolean gates in slime mould (http://arxiv.org/abs/1607.02168).
35. Davydov A. 1979 Solitons, bioenergetics, and the mechanism of muscle contraction. *Int. J. Quantum Chem.* **16**, 5–17. (doi:10.1002/(ISSN)1097-461X)
36. Sirenko YM, Stroscio MA, Kim K. 1996 Dynamics of cytoskeletal filaments. *Phys. Rev. E* **54**, 1816. (doi:10.1103/PhysRevE.54.1816)
37. Pokorný J, Jelínek F, Trkal V, Lamprecht I, Hölzel R. 1997 Vibrations in microtubules. *J. Biol. Phys.* **23**, 171–179. (doi:10.1023/A:1005092601078)
38. Pokorný J. 2004 Excitation of vibrations in microtubules in living cells. *Bioelectrochemistry* **63**, 321–326. (doi:10.1016/j.bioelechem.2003.09.028)
39. Satarić M, Bednar N, Satarić B, Stojanović G. 2009 Actin filaments as nonlinear rlc transmission lines. *Int. J. Mod. Phys. B* **23**, 4697–4711. (doi:10.1142/S021797920905331X)
40. Sekulić DL, Satarić BM, Tuszynski JA, Satarić MV. 2011 Nonlinear ionic pulses along microtubules. *Eur. Phys. J. E* **34**, 49. (doi:10.1140/epje/i2011-11049-0)
41. Priel A, Tuszyński J. 2008 A nonlinear cable-like model of amplified ionic wave propagation along microtubules. *Europhys. Lett.* **83**, 68004. (doi:10.1209/0295-5075/83/68004)
42. Kučera O, Havelka D, Cifra M. 2017 Vibrations of microtubules: physics that has not met biology yet. *Wave Motion* **72**, 13–22. (doi:10.1016/j.wavemoti.2016.12.006)
43. Goulielmakis E *et al.* 2008 Single-cycle nonlinear optics. *Science* **320**, 1614–1617. (doi:10.1126/science.1157846)
44. Baltuška A *et al.* 2003 Attosecond control of electronic processes by intense light fields. *Nature* **421**, 611–615. (doi:10.1038/nature01414)
45. Nabekawa Y, Okino T, Midorikawa K. 2017 Probing attosecond dynamics of molecules by an intense a-few-pulse attosecond pulse train. In *31st Int. Congress on High-Speed Imaging and Photonics, Int. Society for Optics and Photonics*, p. 103280B. International Society for Optics and Photonics.
46. Ciappina MF *et al.* 2017 Attosecond physics at the nanoscale. *Rept. Progr. Phys.* **80**, 054401. (doi:10.1088/1361-6633/aa574e)
47. Jelínek F, Cifra M, Pokornỳ J, Vaniš J, Šimša J, Hašek J, Frỳdlová I. 2009 Measurement of electrical oscillations and mechanical vibrations of yeast cells membrane around 1 kHz. *Electromagn. Biol. Med.* **28**, 223–232. (doi:10.1080/15368370802710807)
48. Cifra M, Vanis J, Kucera O, Hasek J, Frydlova I, Jelinek F, Saroch J, Pokorny J. 2007 Electrical vibrations of yeast cell membrane. *PIERS Online* **3**, 1190–1194. (doi:10.2529/PIERS070220101159)